

# MRF- Clutch - Design Considerations and Performance

D. Lampe, A. Thess, C. Dotzauer  
Dresden University of Technology, Dresden, Germany

## Abstract:

The paper is aimed at design and testing of a Magnetorheological Fluid (MRF) clutch with low idle and high transmittable torque, good long term stability and simple construction. Starting from the basic description of MRF as Bingham Plastics and using the model of different static and dynamic yield stresses, equations for transmitted torque are derived and used to evaluate 'bell'- and 'disc'-shaped clutches. The problem of particle centrifuging is addressed by deriving a nondimensional characteristic parameter for 'disc'-shaped clutches. This parameter clearly specifies the influence of different variables on the stability against demixing of MRF. A new friction- and wearless permanent magnet seal for MRF is described. Experimental results concerning transmitted torque are presented.

## Introduction

Magnetorheological Clutches are distinguished by very good controllability of transmitted torque, very short reaction times and little wearout. The fundamental advantage over traditional clutches consists in their ability to process electric control information directly, i.e. without any mechanical links. Due to several unresolved problems, MRF- clutches could not reach large scale employment yet. This papers goal is to overcome some of those problems.

### Transition between Solid and Liquid State

It is well known that MRF behave in the liquid state like Bingham plastics:

$$\mathbf{t} = \mathbf{t}_0 + \mathbf{h}\dot{\mathbf{g}} \quad (1)$$

with:  $\mathbf{t}$  - shear stress ;  $\mathbf{h}$  - dyn. viscosity

$\mathbf{t}_0$  - yield stress ;  $\dot{\mathbf{g}}$  - shear velocity

The transition from the solid to the liquid state occurs at a different yield stress (static yield stress  $\mathbf{t}_{y,s}$ ) than the opposite transition (dynamic yield stress  $\mathbf{t}_{y,d}$ ) (see [1]).

Clutches in general should have only a minimum torque change while transitioning from stiff transmission to slipping transmission.

The 'bell shape' and the 'disc shape' are the two basic shapes of a MRF- clutch.

### Disc Shaped Clutches

#### Solid Mode

In solid body torsion the shear stress grows linearly with increasing radius:

$$\mathbf{t}(r) = C \cdot r \quad (2)$$

with:  $r$  - radius ;  $C$  = constant

The boundary condition for the maximum torque is:

$$\mathbf{t}(R_o) = \mathbf{t}_{y,s} \quad (3)$$

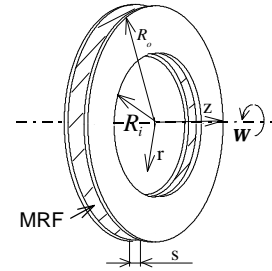


Fig. 1: Sketch of Disc Shape

From eqs. (2) and (3) follows:

$$\mathbf{t}(r) = \mathbf{t}_{y,s} \frac{r}{R_o} \quad (4)$$

The torque transmitted by a differential torus element writes as:

$$dT = \mathbf{t}(r) 2\pi r^2 dr \quad (5)$$

Integration of eq. (5) from  $R_i$  to  $R_o$ , using eq. (4), results in the expression for the maximum in solid mode transmittable torque:

$$T_{\max,stat.} = \pi \mathbf{t}_{y,s} \frac{(R_o^4 - R_i^4)}{2R_o} \quad (6)$$

#### Liquid Mode

For not too large Reynoldsnumbers ( $<10^4$ ) the profile of the azimuthal fluid velocity is linear from one disc to the other, i.e.:

$$\int_z v_{azimuthal}(r, z) = \frac{r(\mathbf{w}_2 - \mathbf{w}_1)}{s} = const. \quad (7)$$

with:  $\mathbf{w}_1$  and  $\mathbf{w}_2$  - ang. velocities of the discs

Introducing eq. (7) into eq. (1) leads to:

$$\mathbf{t}(r) = \mathbf{t}_{y,d} + \mathbf{h}(\mathbf{w}_2 - \mathbf{w}_1) \frac{r}{s} \quad (8)$$

Using eq. (8) to integrate eq. (5) results in the expression for the torque to be transmitted in the liquid mode:

$$T_{dynamic} = \pi \mathbf{t}_{y,d} (R_o^3 - R_i^3) \frac{2}{3} + \pi \mathbf{h} \frac{(\mathbf{w}_2 - \mathbf{w}_1)}{2s} (R_o^4 - R_i^4) \quad (9)$$

From eq. (9) the limiting torque for vanishing

difference in angular velocity is simply to be derived as:

$$T_{\min,dyn} = \mathbf{p}t_{y,d} (R_o^3 - R_i^3) \frac{2}{3} \quad (10)$$

#### Transition from solid to liquid mode

The transmitted torque jumps during transition from solid to liquid mode: (11)

$$\mathbf{p}t_{y,s} \frac{(R_o^4 - R_i^4)}{2R_o} \Rightarrow \mathbf{p}t_{y,d} (R_o^3 - R_i^3) \frac{2}{3}$$

#### Bell Shaped Clutches

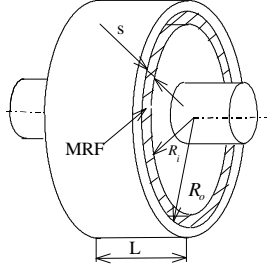


Fig. 2: Sketch of Bell Shape

#### Solid Mode

For not too large gap sizes s the maximum in solid mode transmittable torque is:

$$T_{\max,stat.} = \mathbf{P} \frac{1}{2} (R_o + R_i)^2 L t_{y,s} \quad (12)$$

#### Liquid Mode

The flow between two rotating cylinders with not too large gap size s is a classical problem of fluid mechanics and that is why just the result shall be cited: (13)

$$T_{dynamic} = \mathbf{P} \frac{1}{2} (R_o + R_i)^2 L t_{y,d} + 4\mathbf{p}Lh \frac{(w_2 - w_1) R_o^2 R_i^2}{R_o^2 - R_i^2}$$

with:  $w_1$  and  $w_2$  - ang. vel. of the cylinders  
Taking the limit of eq. (13) for synchronous rotation of both cylinders leads to:

$$T_{\min,dyn} = \mathbf{P} \frac{1}{2} (R_o + R_i)^2 L t_{y,d} \quad (14)$$

#### Transition from solid to liquid mode

The change from solid to liquid mode results in a change of transmitted torque: (15)

$$\mathbf{P} \frac{1}{2} (R_o + R_i)^2 L t_{y,s} \Rightarrow \mathbf{P} \frac{1}{2} (R_o + R_i)^2 L t_{y,d}$$

#### Comparison between Bell- and Disc Shape

Contrary to the disc shape case (11) do  $T_{\min,dyn}$  and  $T_{\max,stat}$  of the bell shape case (15) have the same dependency on the geometrical parameters of the clutch. Hence, because  $t_{y,s}$  and  $t_{y,d}$  are given and not of equal magnitude, there will always be an unwanted torque jump during transition from solid to liquid mode and vice versa.

For the disc shape, on the other side, a torque jump can be avoided by means of reasonably choosing the inner and the outer radius.

#### Particle Centrifuging

Particle centrifuging is of special interest when running the MRF-clutch idle i.e. no magnetic field is applied. In this case one side is rotating and the other one does not. All other relevant cases can be assumed to have a strong enough magnetic field to prevent the particles from moving outward.

At higher Reynoldsnumbers a circulating fluid motion exists. This causes a zone with radially inward directed fluid velocity at the non rotating side.

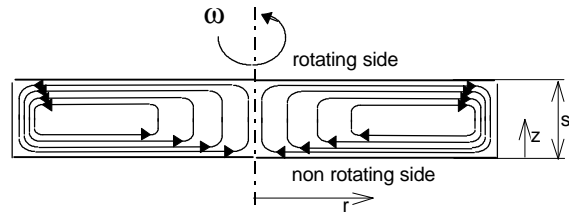


Fig. 3: Circulating Fluid Motion

For this inward motion to be strong enough to make a particle moving inward, the velocity drag on the particle has to be larger than the centrifugal force acting on it.

For spherical particles the centrifugal force is:

$$F_c = \frac{4}{3} \mathbf{p} R_p^3 (\mathbf{r}_p - \mathbf{r}_f) r w_{local}^2 \quad (16)$$

with:  $R_p$  - particle radius;  $\mathbf{r}_p$  - particle density

$\mathbf{r}_f$  - base fluid density;  $w_{local}$  - local ang. vel.

The local angular velocity can be approximated as linearly increasing from the non rotating to the rotating side:

$$w_{local} = w \frac{z}{s} \quad (17)$$

Yielding for eq. (16) :

$$F_c = \frac{4}{3} \mathbf{p} R_p^3 (\mathbf{r}_p - \mathbf{r}_f) r \left( \frac{z}{s} \right)^2 w^2 \quad (18)$$

Stokes' equation describes the drag on a small slowly moving spherical particle:

$$F_d = 6\mathbf{p} R_p \mathbf{h}_f (u_p - u_M) \quad (18)$$

with:  $\mathbf{h}_f$  - dynamic viscosity of base fluid

$u_p$  - radial particle vel. ;  $u_M$  - radial MRF vel.

Ref. [2] gives the following equation as 1st approximation for the radial velocity  $u_M$  : (19)

$$u_M = -rz \left( \frac{w}{s} \right)^2 \frac{2}{\mathbf{n}_M} \left[ \frac{s^3}{30} - \frac{3}{40} s^2 z + \frac{z^3}{24} \right]$$

with:  $\mathbf{n}_M$  - kinematic viscosity of MRF

Equation (19) can be transformed to:

$$u_M = \frac{-rs^2 \mathbf{w}^2}{\mathbf{n}_M} X \quad (20)$$

$$\text{with: } X = \left[ \frac{1}{15} \left( \frac{z}{s} \right) - \frac{3}{20} \left( \frac{z}{s} \right)^2 + \frac{1}{12} \left( \frac{z}{s} \right)^4 \right]$$

Introducing eq. (20) into eq. (18), setting the centrifugal force equal to the drag force and rearranging for particle velocity leads to:

$$\frac{u_p}{r\mathbf{w}^2} = \frac{2}{9} R_p^2 \frac{(\mathbf{r}_p - \mathbf{r}_f)}{\mathbf{h}_f} \left( \frac{z}{s} \right)^2 - \frac{s^2}{\mathbf{n}_M} X \quad (21)$$

In order to generalize, we define a nondimensional particle velocity:

$$U = u_p \frac{\mathbf{n}_M}{rs^2 \mathbf{w}^2} \quad (22)$$

Using this nondimensional particle velocity, equation (21) becomes:

$$U = \left\{ \left( \frac{R_p}{s} \right)^2 \frac{\mathbf{n}_M (\mathbf{r}_p - \mathbf{r}_f)}{\mathbf{h}_f} \right\} \left\{ \frac{2}{9} \left( \frac{z}{s} \right)^2 \right\} - X \quad (23)$$

Equation (23) is of the kind:

$$U = A \cdot g(\mathbf{x}) - f(\mathbf{x}) \quad (24)$$

with:  $\mathbf{x} = \frac{z}{s}$

The variable A can be interpreted as *characteristic parameter* of the nondimensional particle velocity:

$$A = \left( \frac{R_p}{s} \right)^2 \frac{\mathbf{n}_M (\mathbf{r}_p - \mathbf{r}_f)}{\mathbf{h}_f} \quad (25)$$

Eq. (25) shows that an increase of gap size  $s$  as well as a reduction of the particle radius  $R_p$  would result in a quadratic improvement of the characteristic parameter A.

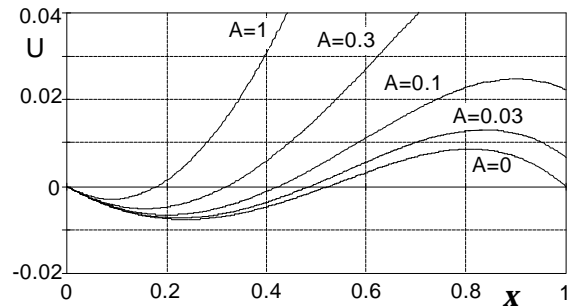


Fig. 4: nondim. particle velocity vs. nondim. distance to the non rotating disc

In Fig. 4 positive velocities mean outward moving particles and negative velocities stand for inward directed particle motion. For good mixing the inward flow should be pronounced.

The outward directed particle flux  $O$  computes as follows:

$$O(A) = \sqrt{\int_0^1 U^2(\mathbf{x}, A) d\mathbf{x}} + \int_0^1 U(\mathbf{x}, A) d\mathbf{x} \quad (26)$$

Whereas the inward directed particle flux  $I$  can be written as:

$$I(A) = \sqrt{\int_0^1 U^2(\mathbf{x}, A) d\mathbf{x}} - \int_0^1 U(\mathbf{x}, A) d\mathbf{x} \quad (27)$$

The ratio between the inward and the outward directed particle flux shall be defined as 'quality factor'  $y$ :

$$y(A) = I/O \quad (28)$$

Integration of eqs. (26) and (27) leads to Fig. 5:

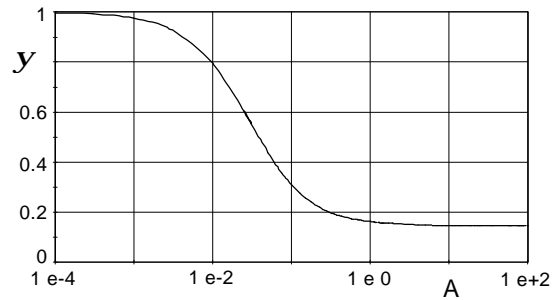


Fig. 5: Quality Factor vs. Characteristic Parameter

$\psi=1$  means that as many particles move inward as particles are floating outward, i.e. no settling will occur. The smaller  $\psi$  becomes, the faster demixing will take place.

Fig. 5 also shows that A has to be at least  $< 0.1$  in order to get an improvement in stability against particle settling due to centrifugal forces.

The following example is included to demonstrate, how the gap size  $s$  can influence the characteristic parameter A.

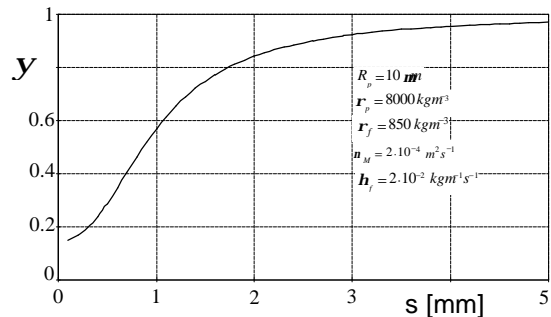


Fig. 6: Example of Quality Factor vs. Gap Size

Fig. 6 shows for typical values that an increase in gap size from, for example, 0.5 mm to 2.5 mm will result in a remarkable improvement of stability against particle demixing.

## Test Clutch

A test clutch of the following design was built:

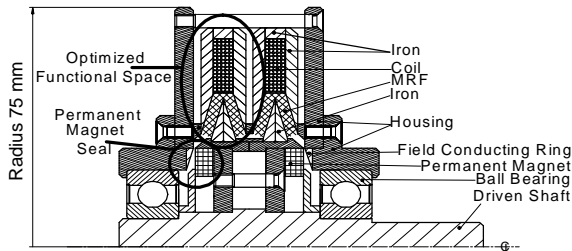


Fig. 7: Test Clutch

For this test clutch a dihedral disc shape was chosen. By this means the only to idle torque contributing disc area was minimized and the whole Functional Space became smaller in size. The optimum V-angle was computed with a special FORTRAN-program in order to provide for optimum magnetic flux in the iron parts. Furthermore, the V-shape contributes to a significant reduction in wall thickness, which is highly advantageous for better heat transfer from the MRF.

The heating problem was also addressed by making the driving side the outer side, hence when the clutch is rotating, the cooling will be driven by turbulent air flow over the rotating outer housing.

For sealing purposes a permanent magnet seal was developed. It employs the MRF's magnetizability in order to exert a magnetic pressure. This magnetic pressure is generated by a permanent magnet and prevents the MRF from leaking during standstill of the clutch. In the test clutch a pressure height of about 2350 Pa (77mm) has to be overcome. The used permanent magnetic rubber *Fehrenkemper ms 1-Flexo 150* has a coercive field strength of 158 kA/m. Fig. 8 shows the computed magnetic pressure for the test clutch filled with MRF 132 LD of LORD Corp. using provided magnetization curves for the MRF. Computations were made with OPERA-2D.

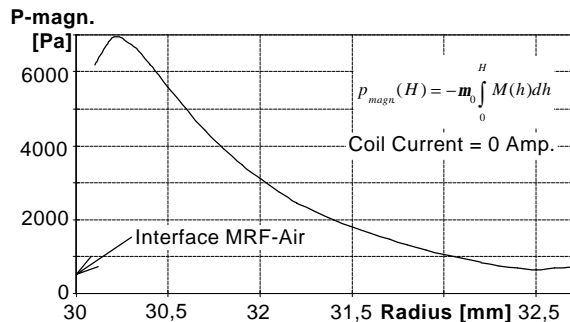


Fig. 8: Computed Magnetic Pressure vs. Radius

## Performance:

The following figures shall give a short overview over the measured performance of the test clutch (Fig. 7). MRF 132 LD of LORD Corp. was used.

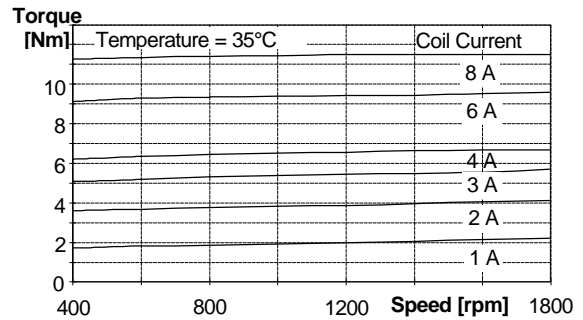


Fig. 9: Torque vs. Speed

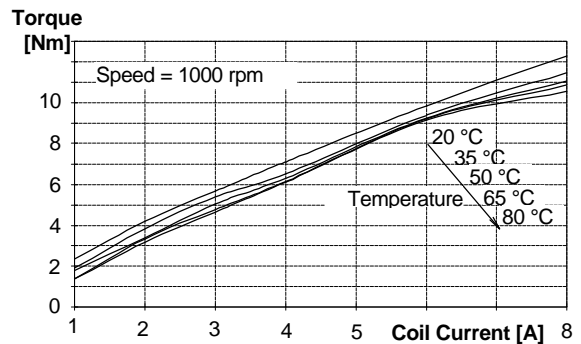


Fig. 10: Torque vs. Coil Current

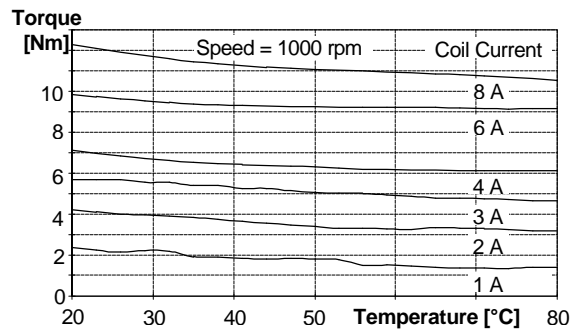


Fig. 11: Torque vs. Temperature

## References

- [1] Weiss, K.D., Material aspects of electrorheological systems, Journal of Intelligent Material Systems and Structures, Volume 4, Iss.1, 1993
- [2] Schultz-Grunow, Der Reibungswiderstand rotierender Scheiben in Gehäusen, Ztschr. f. angew. Math. und Mech. vol. 15, iss. 4, 1935